Data Table 3 Anatase, TiO_2 (12)

Tetragonal, space group $I4_1/amd$, No. 141; $a = 3.785$, $c = 9.515$ Å; $Z = 4$, $V = 136.31$ Å^3

Atomic Positions

Ti in 4(a): 0,0,0; 0,$\frac{1}{2}$,$\frac{1}{4}$; bc

O in 8(e): 0,0,z; 0,0,$\bar{z}$; 0,$\frac{1}{2}$,$z + \frac{1}{4}$; 0,$\frac{1}{2}$,$\frac{1}{4} - z$; bc; $z = 0.2066$

Atomic Distances

Ti–O = 1.89_3 Å (4×), 1.96_6 Å (2×); mean = 1.91_7 Å

RUTGERS

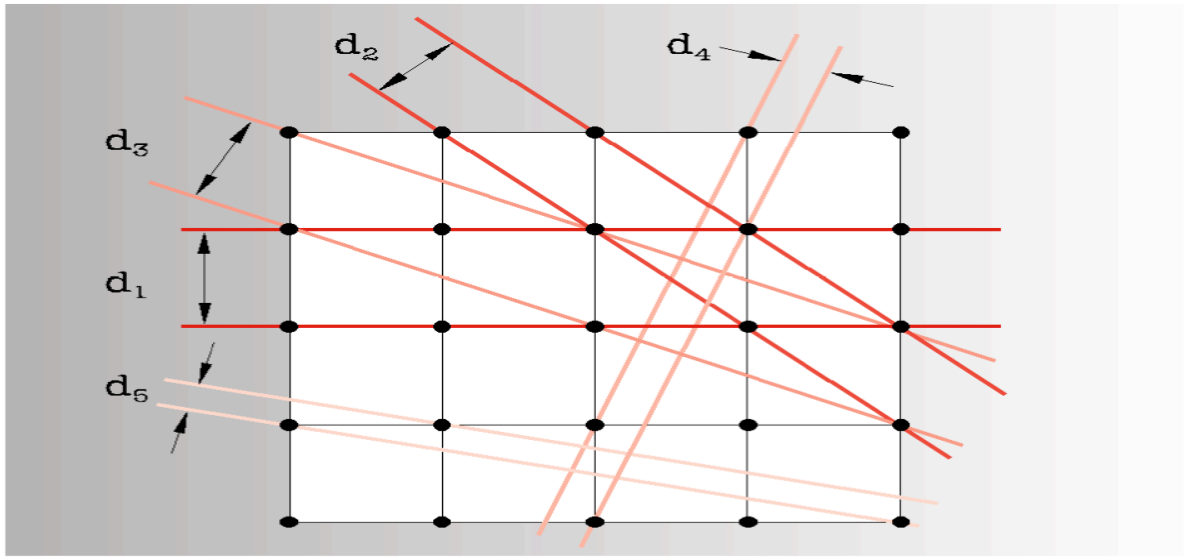
d_2
d_4
d_3
d_1
d_5

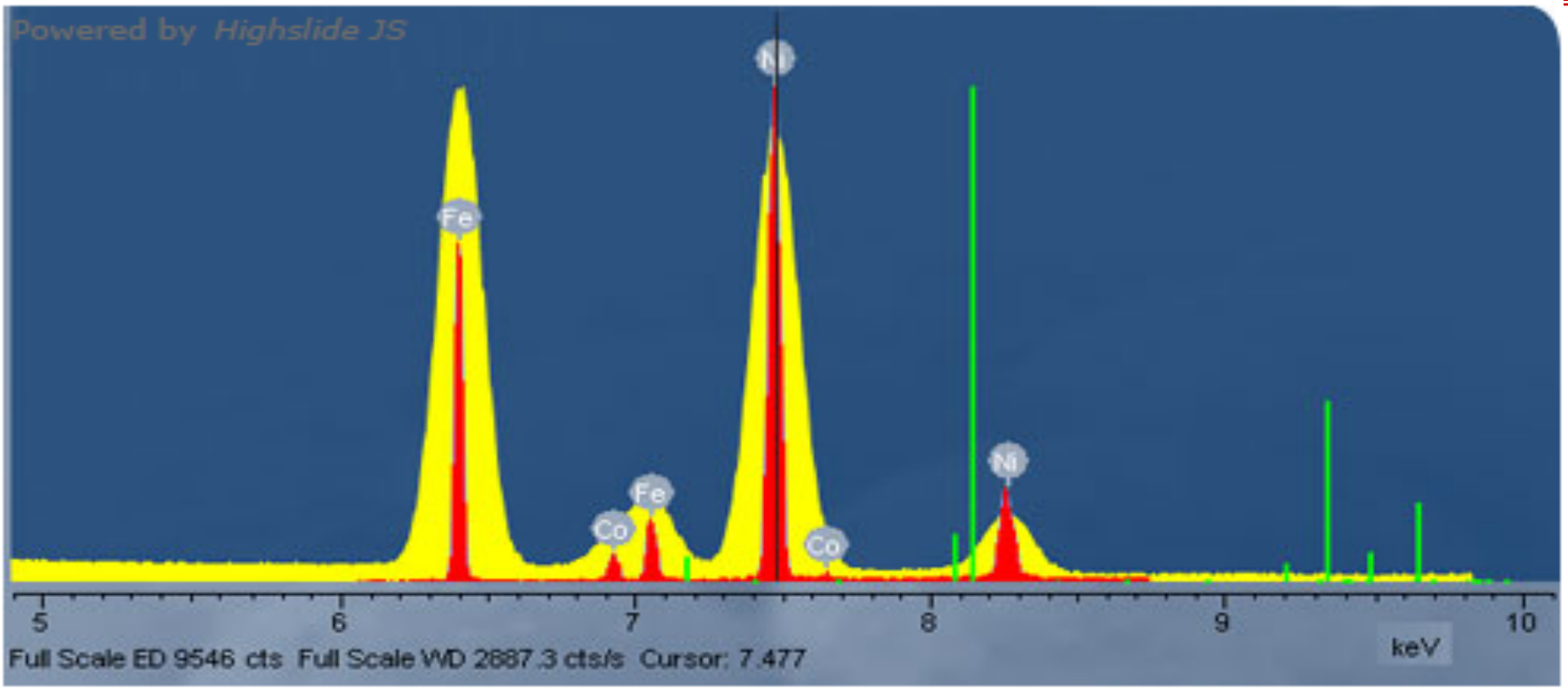

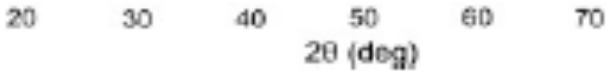

WD-XRF (WDX) vs EDS of Tool Steel

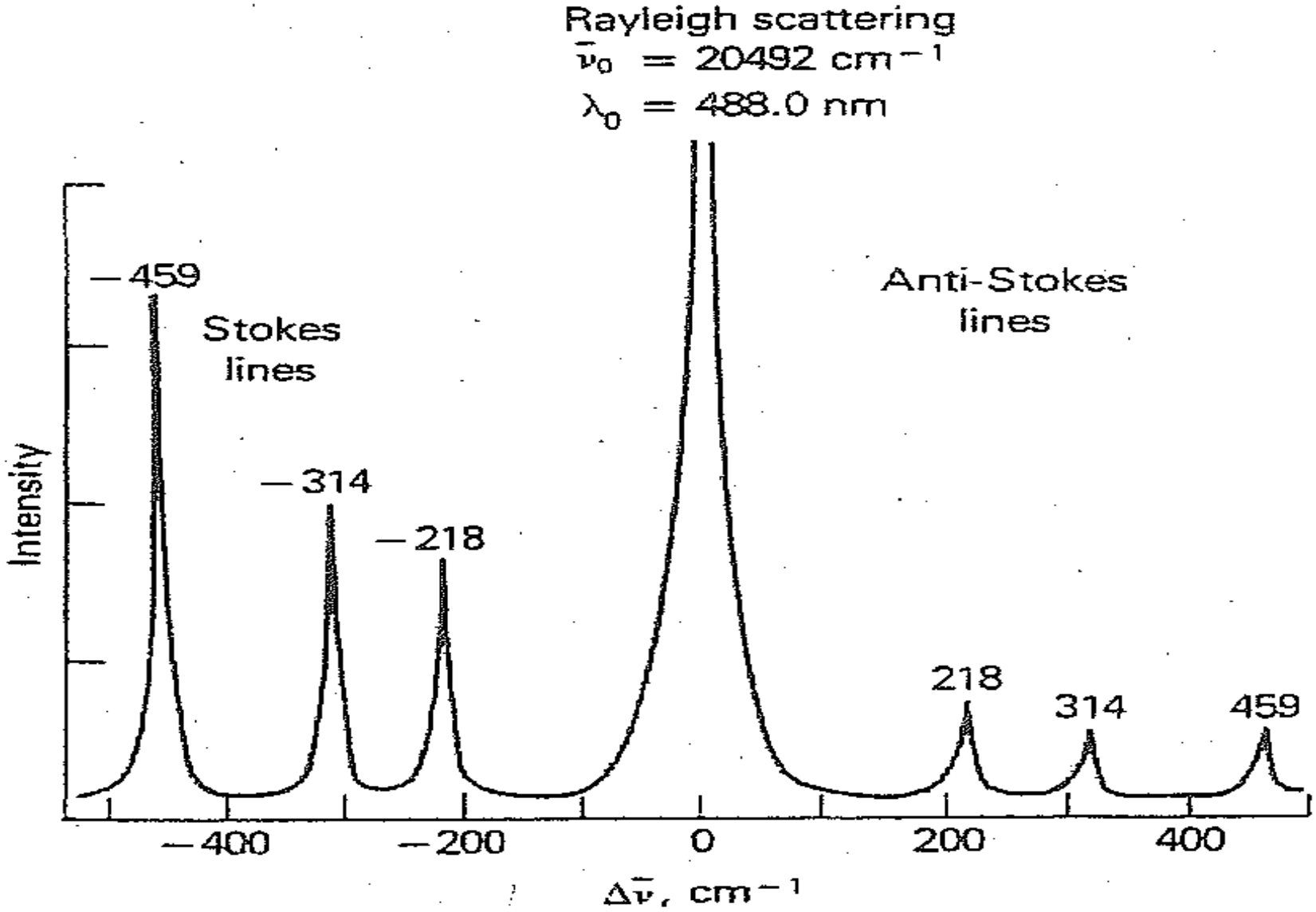

IGURE 13–1 Raman spectrum for CCl_4 excited by lase

RUTGERS

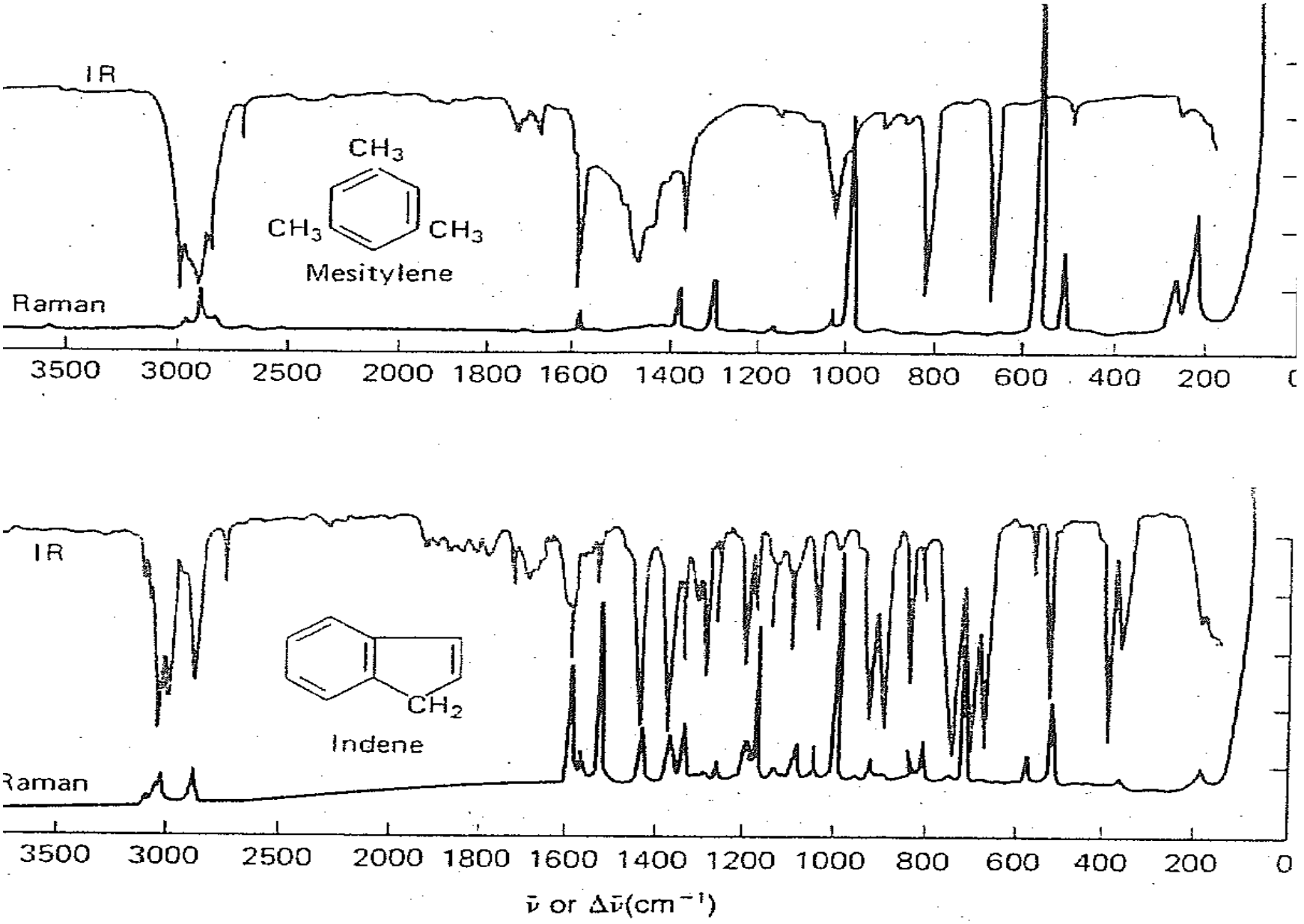

13–3 Comparison of Raman and infrared spectra. (Courtesy Perkin-Elmer

RUTGERS

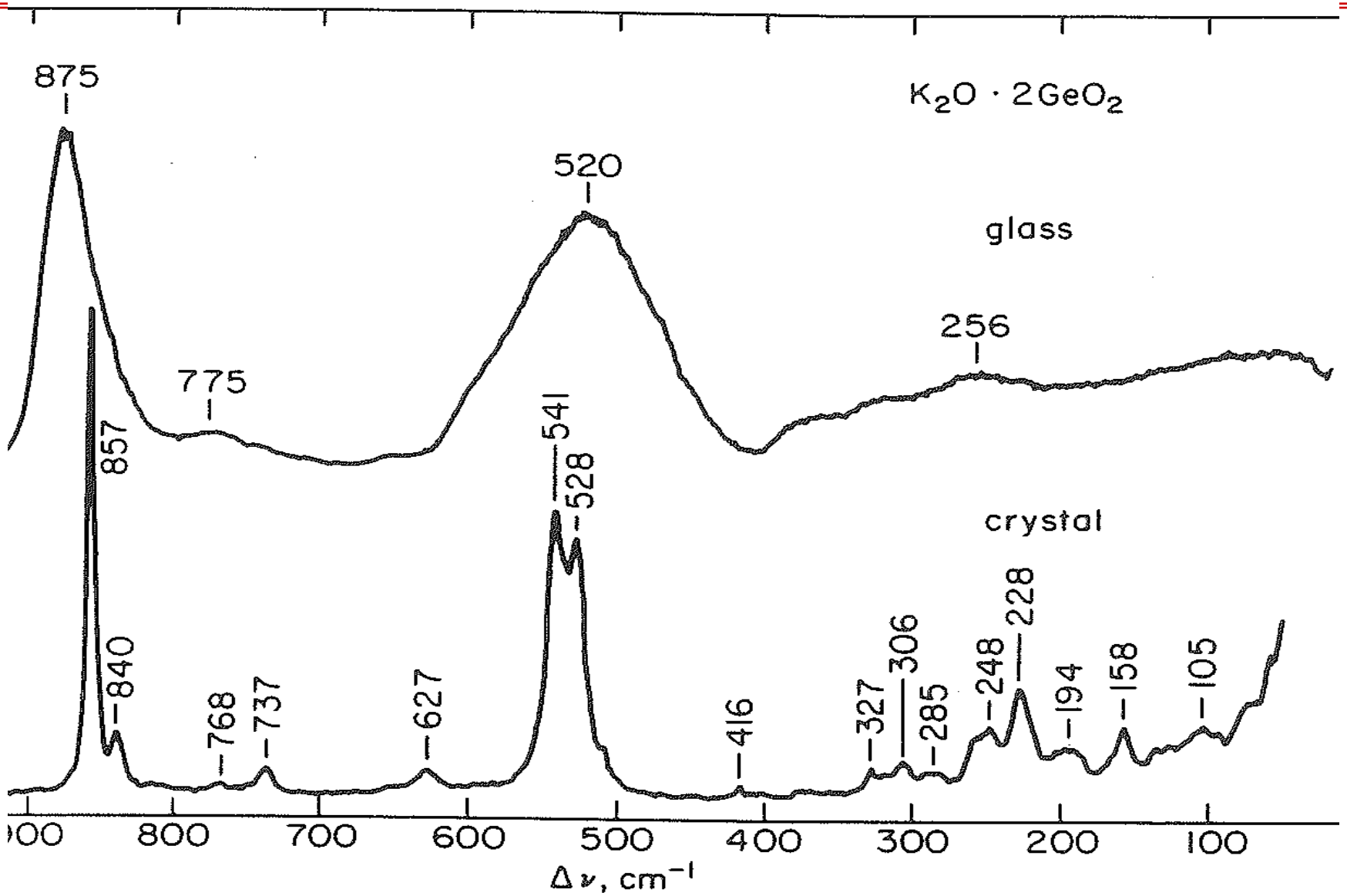

Raman spectra of crystalline and glassy potassium digermanate sho comparison between crystal spectra and glass spectra.

HRTEM studies often show thin IGFs in polycrystalline ceramics

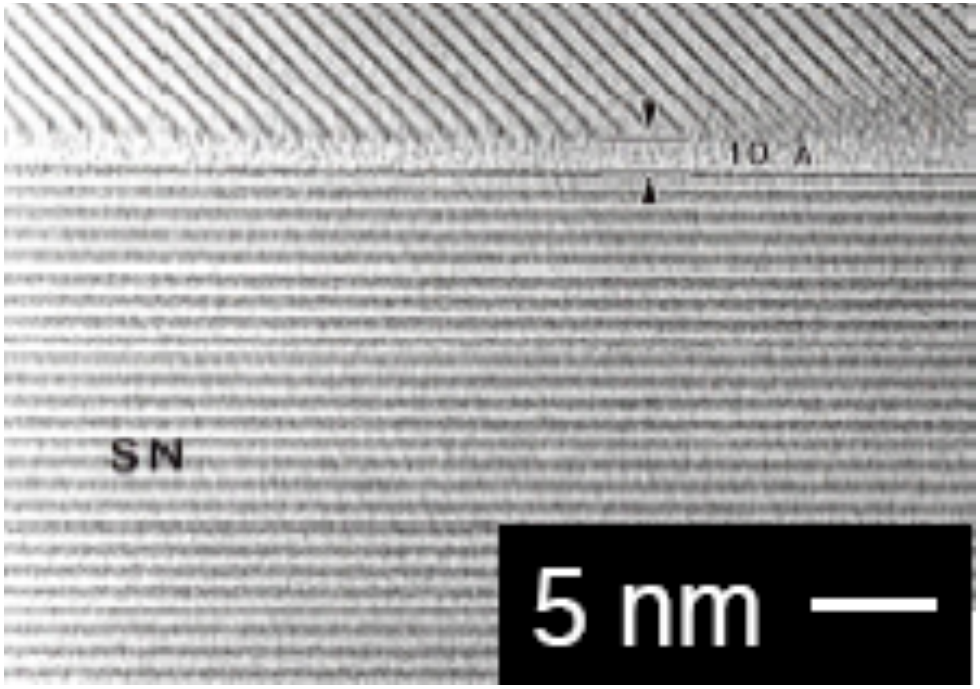

Kleebe, et al, JACerS 76(1993)1969

THIS AMORPHOUS IGF COMES FROM IMPURITIES THAT SEGREGATE TO SURFACES OR FROM ADDITIVES USED AS SINTERING AIDS

WHILE IGFs MAKE UP ONLY A SMALL VOLUME % OF A MATERIAL, THEY CAN STRONGLY INFLUENCE MATERIAL PROPERTIES (SUCH AS MICROSTRUCTURE, MECHANICAL PROPERTIES, CORROSION, AND ELECTRICAL PROPERTIES)

CHANGE OF ONE SPECIES IN THE IGF COMPOSITION CAN CHANGE FRACTURE BEHAVIOR

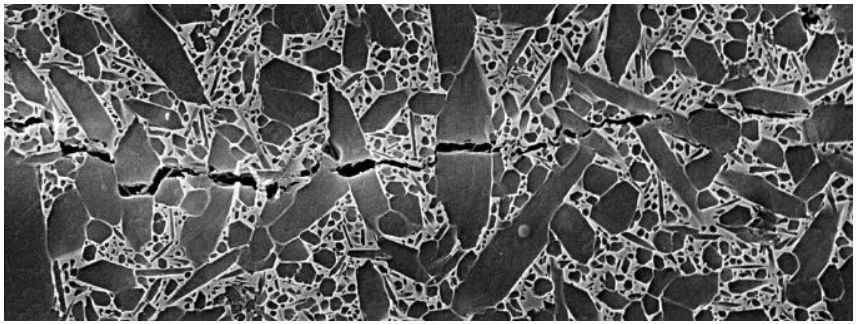

Transgranular fracture
Lu in IGF

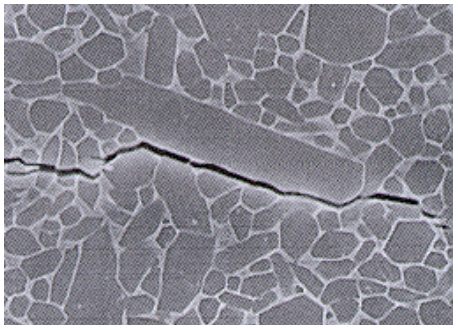

Intergranular fracture
La in IGF

Properties can be significantly affected by the atomistics of the IGF

Growth ratio

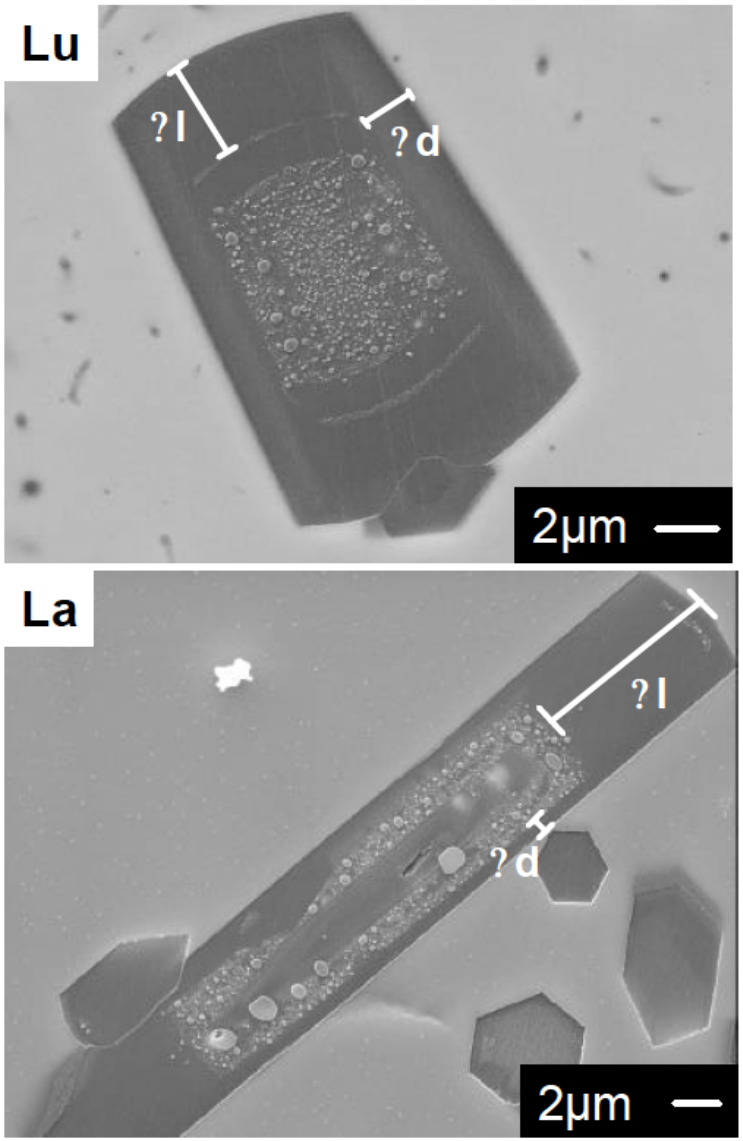

Satet et al. NANOAM

RUTGERS

Lu on Silicon Nitride prism surface (HAADF-STEM)

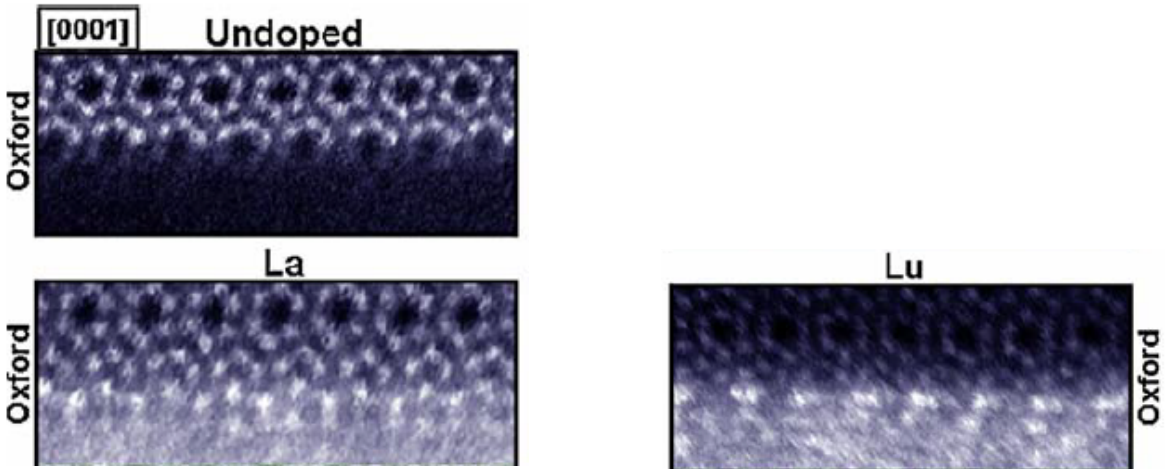

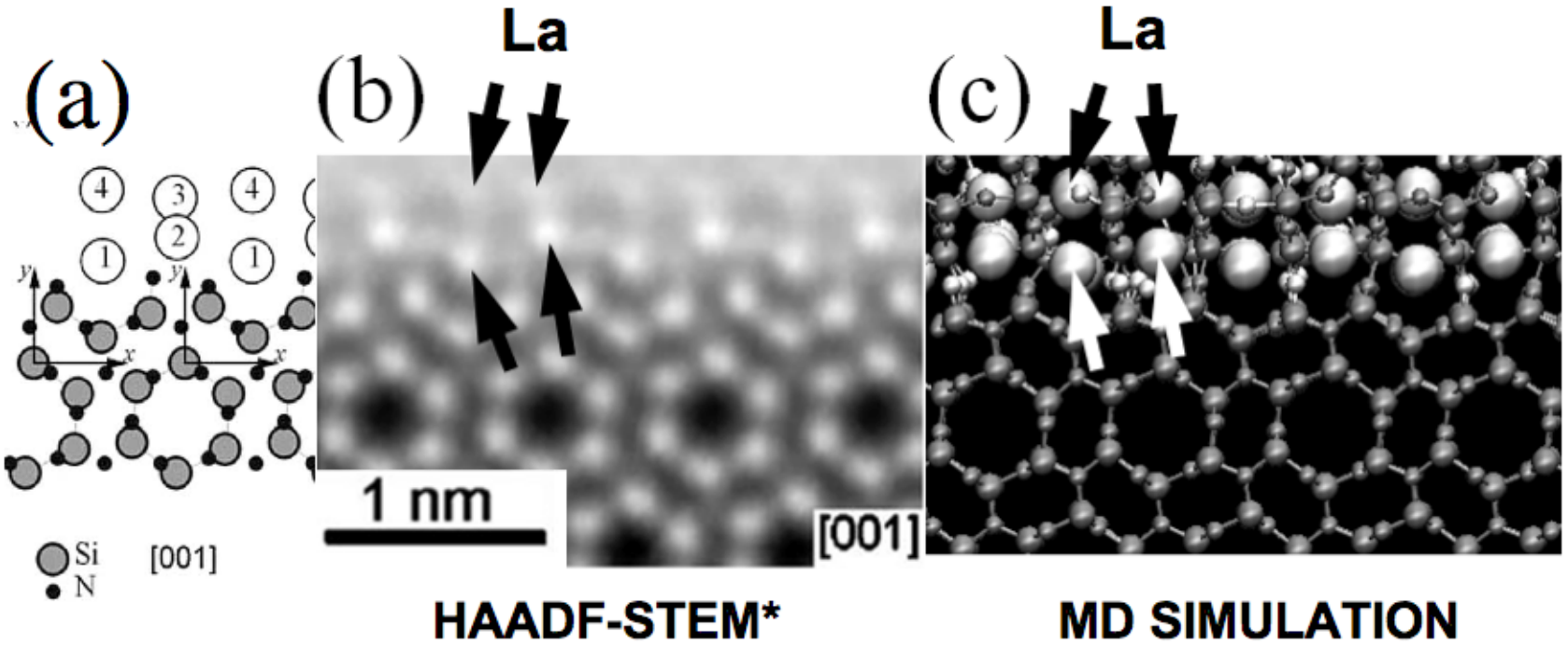

*Winkelman et al. APL 2005

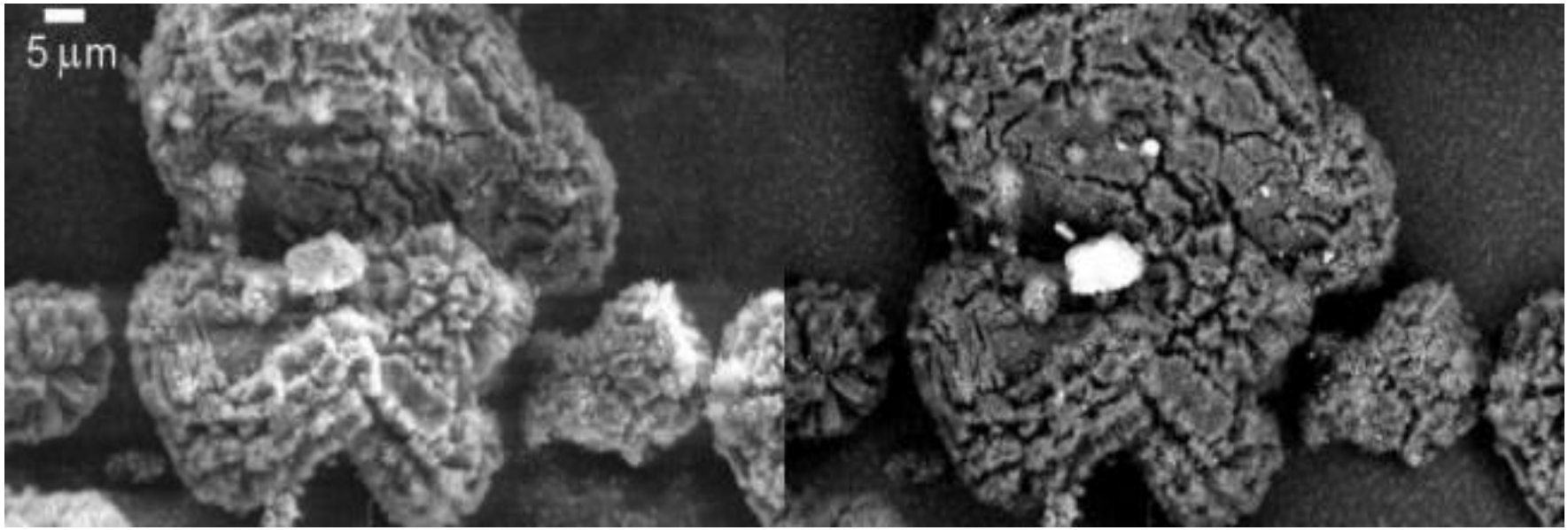

SEM images of Fe particles in carbon recorded with the secondary electron (left) and the back-scattered (right) electron detector. The BSE image shows the Fe particles with bright contrast.

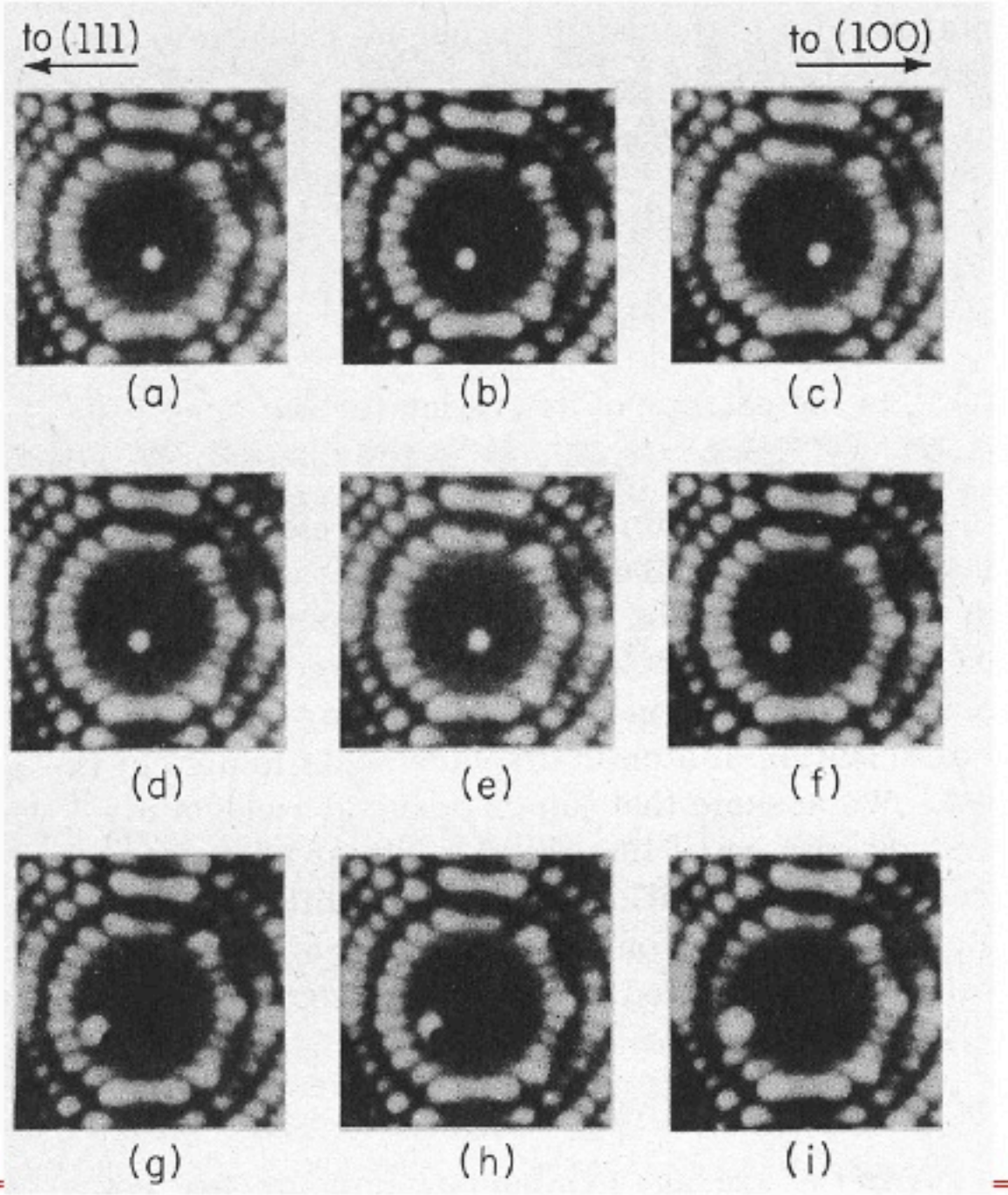

RUTGERS

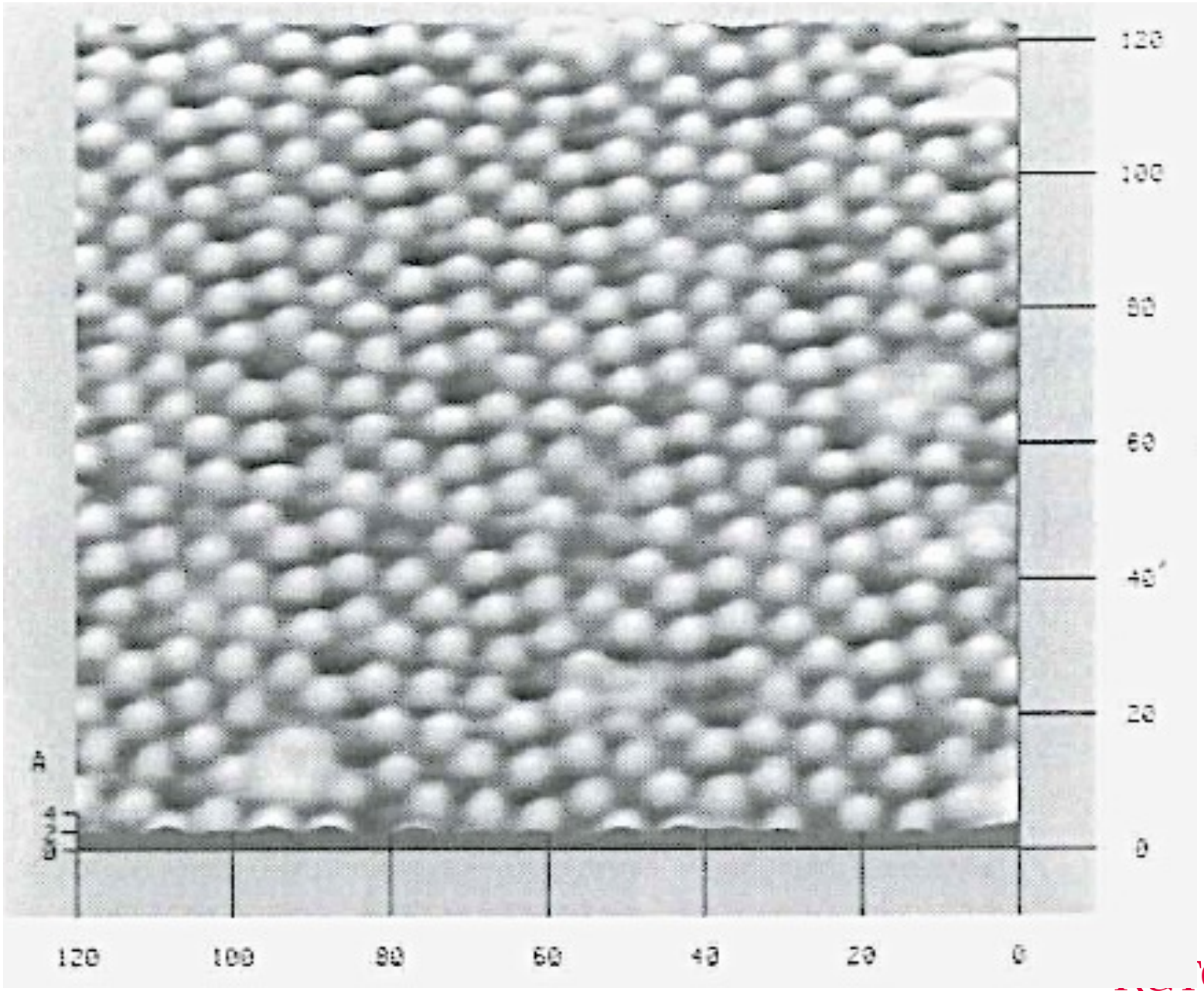

RUTGERS

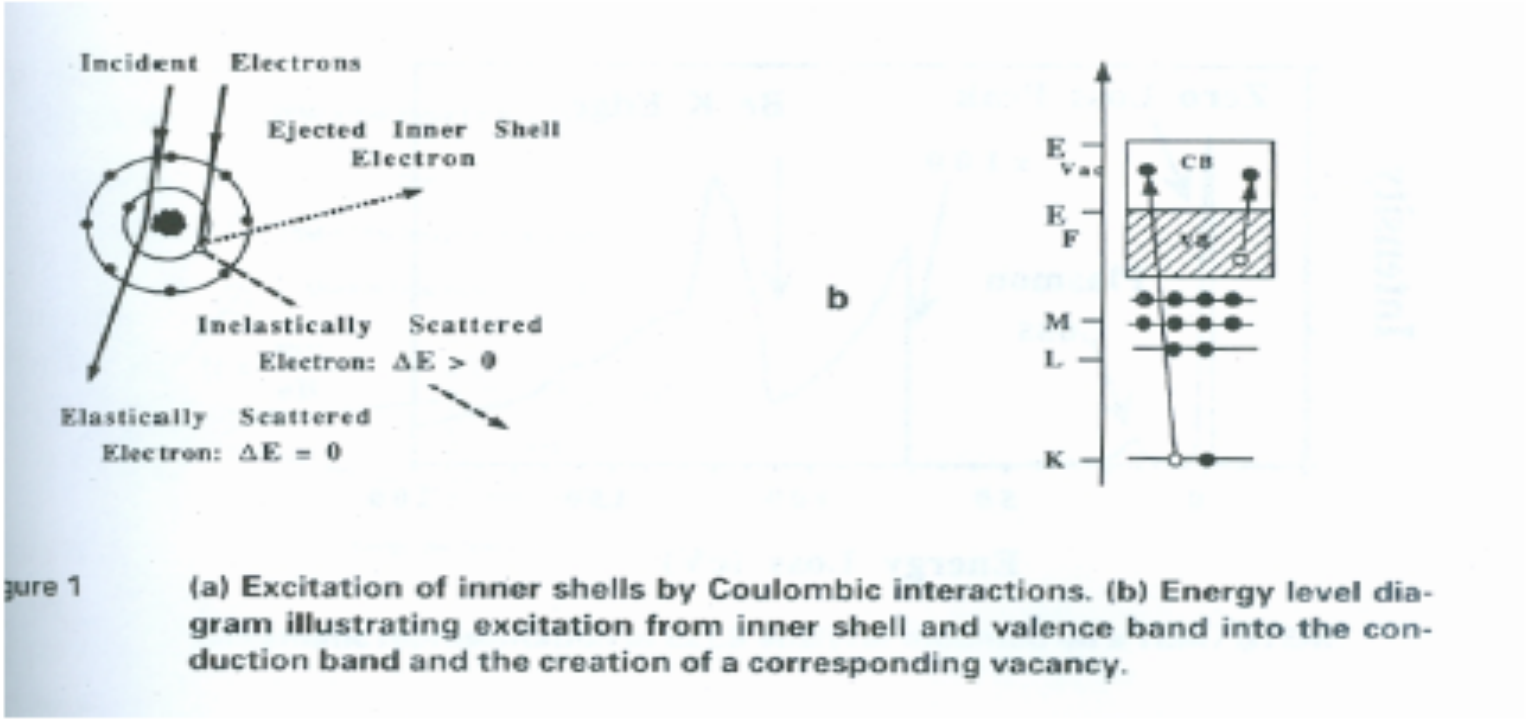

gure 1 (a) Excitation of inner shells by Coulombic interactions. (b) Energy level diagram illustrating excitation from inner shell and valence band into the conduction band and the creation of a corresponding vacancy.

EELS mechanism

RUTGERS

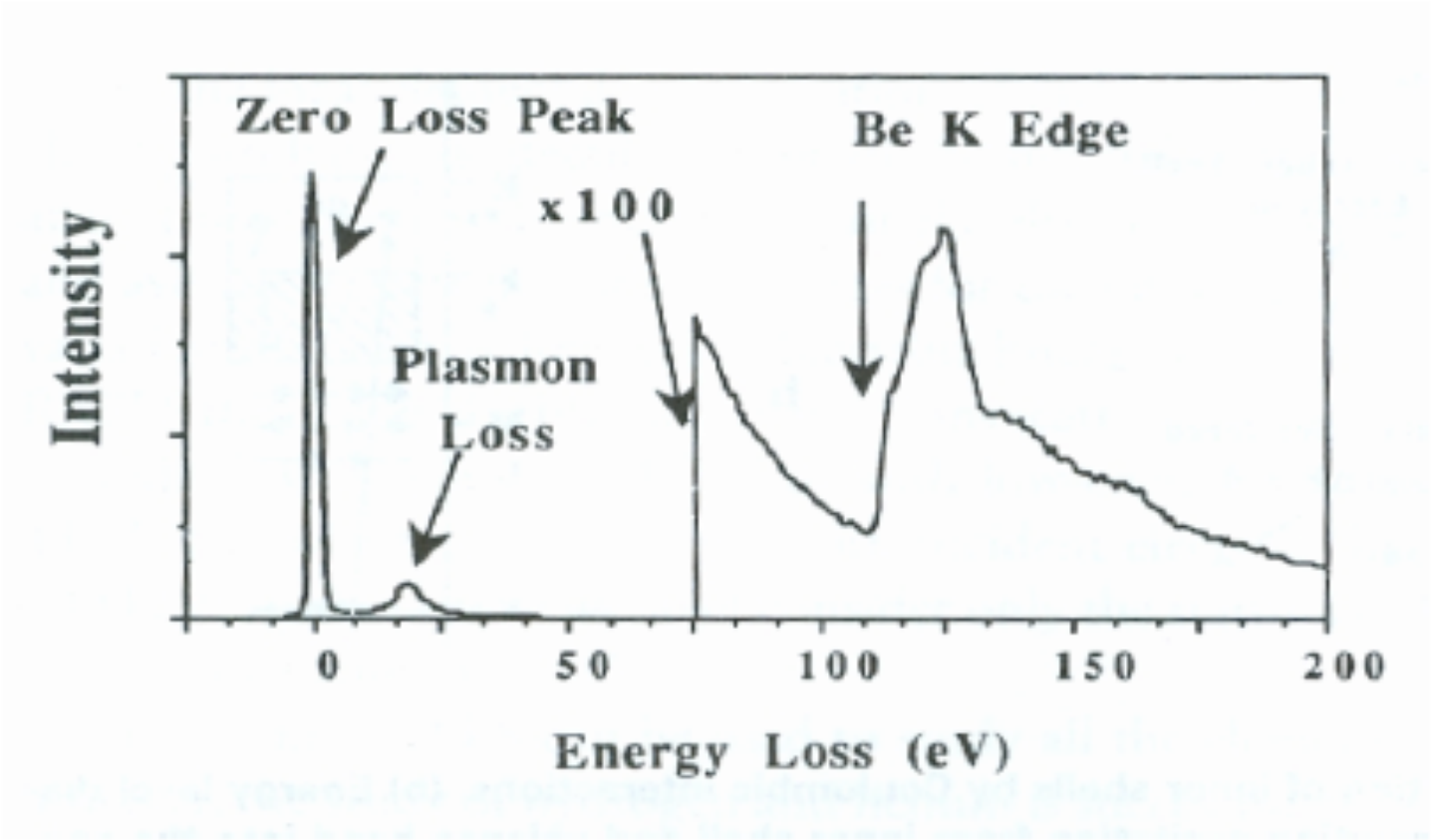
Zero Loss Peak
Be K Edge
x100
Plasmon
Loss
Intensity
0
50
100
150
200
Energy Loss (eV)

EELS

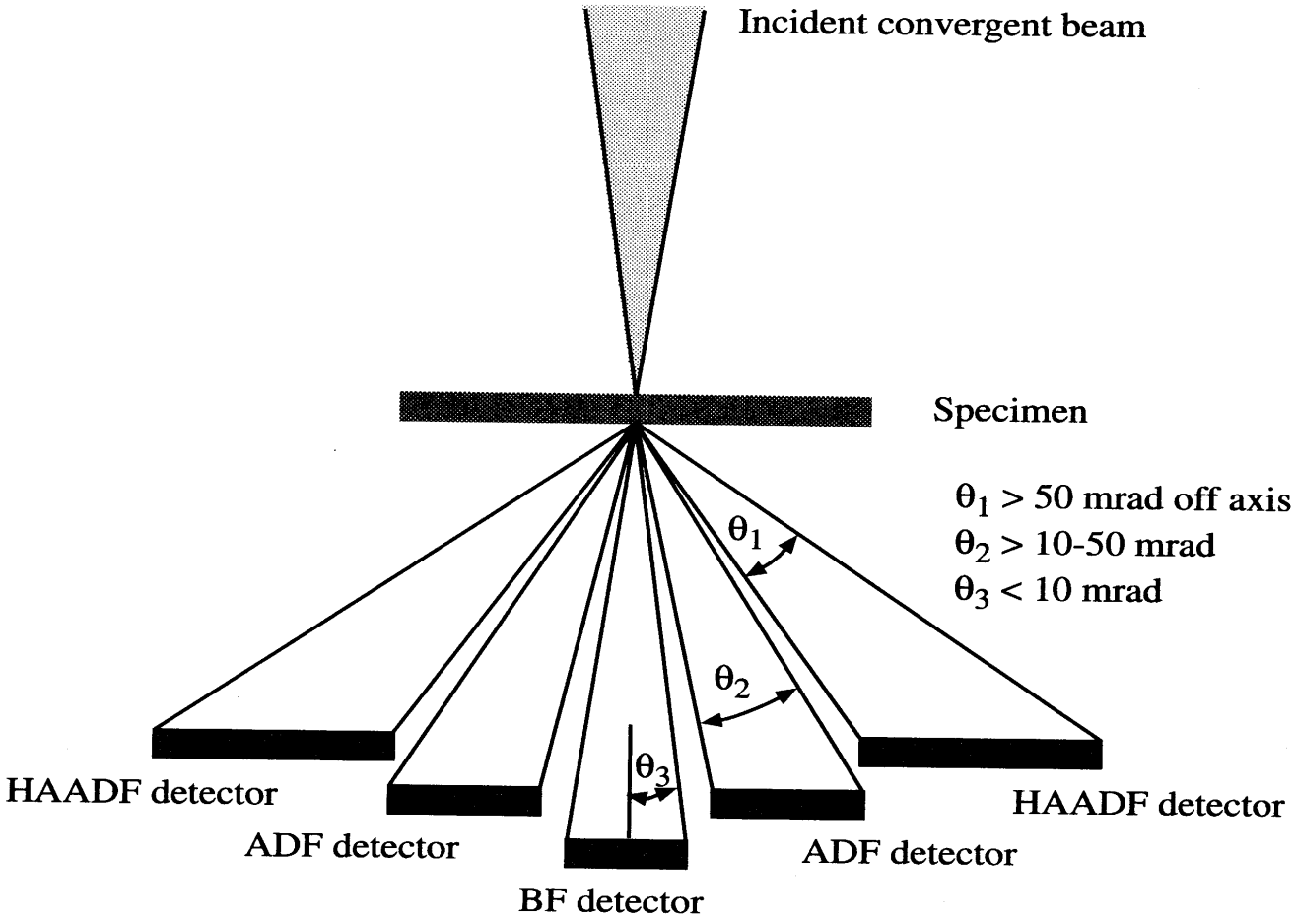
Incident convergent beam
Specimen
θ1 > 50 mrad off axis
θ2 > 10-50 mrad
θ3 < 10 mrad
θ1
θ2
θ3
HAADF detector
ADF detector
BF detector
ADF detector
HAADF detector

Effect of

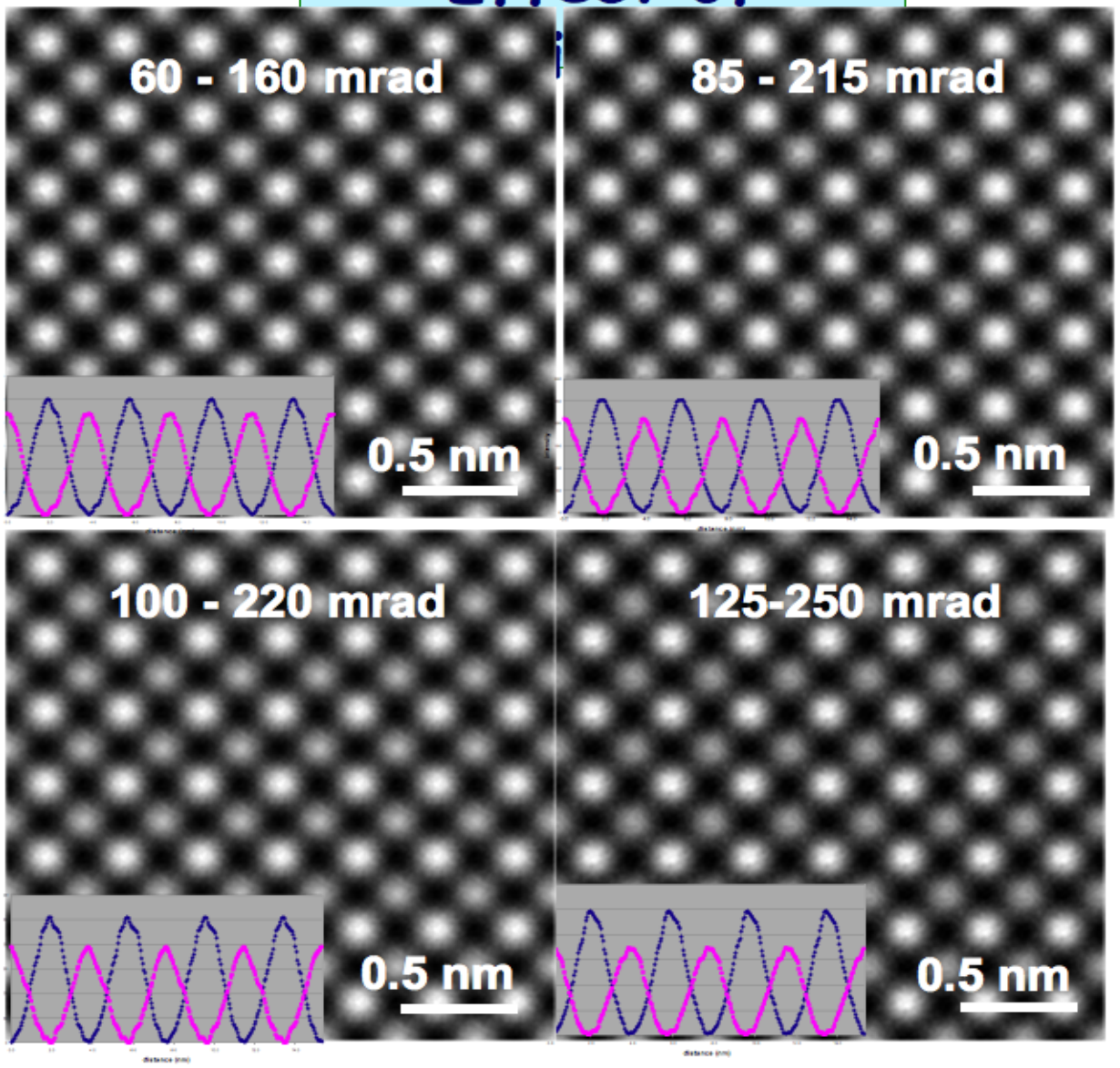
60 - 160 mrad
0.5 nm
85 - 215 mrad
0.5 nm
100 - 220 mrad
0.5 nm
125-250 mrad
0.5 nm